

## A CAD tool for RF MEMS devices

Rajesh Pande

Dept. of Electronics and  
computer science  
Visvesvaraya National  
Institute of Technology  
Nagpur, INDIA-440011  
Tel : 91-9822224468  
Fax : 91-712-2583237  
e-mail:  
panderaj@yahoo.com

Rajendra Patrikar

Dept. of Electronics and  
computer science  
Visvesvaraya National  
Institute of Technology  
Nagpur, INDIA-440011  
Tel : 91-9890124732  
Fax : 91-712-2583237  
e-mail:  
rajendra@computer.org

**Abstract-** A stable, multiple energy domain and multi scale simulation tool for Microsystems is developed. A structured design methodology is adopted for design and optimization of RF MEMS shunt switch and MEMS inductor. The CAD tool developed is a device specific and incorporates physical parameters such as surface roughness. The tool analyzes the impact of surface roughness and also does thermal analysis. These are useful for understanding reliability and failure mechanisms of RF MEMS components.

### I. Introduction

Computer Aided Design (CAD) systems for MicroElectroMechanicalSystems (MEMS) require the three dimensional modeling to take into accounts all the domain characteristics. At present, commercially available CAD tools are not sufficient to model all the parasitic effects, which dominate the electrical or mechanical properties. For example most of the surfaces are represented by smooth topologies in these tools and in reality most of the surfaces are rough. The micro roughness, which is very important to analyze performance as well as reliability issues needed to be modeled. There are other parameters such as noise which are not calculated in the tools. Unlike CMOS CAD tools it may be necessary to have different tools for each MEMS device since they operate in different domains. Each tool takes into account all the domain characteristics of the device.

The advent of VLSI-compatible MEMS fabrication technologies has led to the development of increasingly complex and integrated MEMS based systems. Most MEMS CAD tools are focusing on device level characteristics. The commercial CAD systems for MEMS design are generic in nature. Hence the available CAD tools are lacking ability to predict design performance and optimization with regard to some of the parasitic effects. For example most of the surfaces are represented by smooth topologies and in reality most of the surfaces are rough. There are other parameters such as noise is also not accounted in generic tools [1]. It is necessary to take into account these surface properties since surface to

volume ratio is increasing for all devices as the dimensions are continuously shrinking. The accurate modeling of the physical properties such as surface topology and its impact on the electrical parameters will help to predict the deviation in performance. For example it is reported that rough surface contact formed between the bridge metal and the isolation layer in the “down” position of the capacitive coupled switches may lead to the discrepancy between the measured and predicted data as high as 40% since the technology is in the inception stage [2] [3]. The device designer needs to understand the device performance with the help of accurate modeling and simulation of device model. This is essential to improve the manufacturability of MEMS devices as seen in silicon technology. The tools are also lacking support to testability. The CMOS circuit technology works mainly in electrical domain as oppose to MEMS devices which have different domains based on the application. Thus it may be necessary that for each MEMS device specialized CAD tool is required, which takes into account all the domain characteristics. The recent efforts in microelectronics and MEMS have shown promising results in realization of high performance passive components for RF applications. However, modeling and simulation of MEMS RF components is quite challenging because of complexity involved.

In the today’s technology, computing electrical parameters such as inductance or capacitance using conventional techniques is no longer being accurate because of miniaturization. At the same time, using highly accurate techniques such as a fine-grained Finite Element Method (FEM) may not be feasible due to the large computation time. Our efforts are focused to develop the tool for RF MEMS shunt capacitive switch and MEMS inductor. The tool also incorporates the ability to analyze the effect of surface roughness on RF MEMS shunt switches and MEMS inductor, which is absent in state of the art MEMS CAD tools. The mechanical analysis of RF MEMS shunt switch is performed by creating FEM model of the structure. The failure mechanism for RF MEMS shunt switch is primarily due to

temperature effects and this tool also analyzes the temperature distribution in the structure. Rest of the paper is organized as follows. In section II CAD framework for MEMS, adopted for this work is discussed. The modeling of MEMS shunt switch is discussed in section III followed by modeling issues of inductor in section IV. In section V temperature analysis for shunt switch is presented followed by summary in section VI.

## II. CAD framework for MEMS devices

A significant progress is made in technology of MEMS devices. In MEMS CAD significant progress has been made, but the current state-of-the-art tools have not yet achieved the maturity what CAD tools have for VLSI. The CAD support is also needed by the MEMS-device or MEMS-system designer. The MEMS-device designer requires an accurate, behavior model that captures all the essential behavior, including parasitic effects and permit predictable design modifications and optimizations. The Rapid, accurate, efficient analysis of many alternatives during the design process is crucial to developing high quality, robust devices and systems. MEMS are miniature electromechanical systems developed from the mature batch-fabricated processes of VLSI technologies. In developing the MEMS design tool, the design process can be considered as combination of EDA (Electronic Design Automation) and MDA (Mechanical Design Automation). The EDA covers partial derivative equations physics solvers, layout and process tools and spice. The MDA includes solid modeling and mesh generation tools, partial derivative equations physics solvers in mechanical domain. The integration of EDA and MDA must also support new design methodologies. Commonly used MEMS design methodology is unstructured design flow. Lack of hierarchy and one-way design flow are the main drawbacks of this methodology. The structured design methodology combines the design of micromechanical and electronics into a single flow in which the MEMS circuit representation plays a central role. The advantages of this approach are reusability of the parametric circuit models and allow quick iteration between system, circuit and layout representations. The structured design environment provides the usability of technology to large scale fabrication. The structured design approach has significantly contributed to the explosive growth of VLSI technology. MEMS design methodologies in wide use today, do not support hierarchical representations suitable for

verification based iterative systems. This methodology adopted from the electronic design techniques enables fast design verification of complex electronic and micro-mechanical designs [4]. Complexity in electronic design is handled through a hierarchy of devices, components and blocks, which can share the same layout representation. EDA tools support this design hierarchy. Due to uniform nature of representation, the designer can use various levels of abstraction. It also helps to make the iterative design process faster. Due to mixed energy domains the MEMS have greater complexity. The generic design flow for MEMS is shown in Fig. 1 [1][4][5][6]. In the design flow of Fig. 1, since the tool developed is intended for RF MEMS shunt switches and MEMS inductors only, the technology information is passed to schematic and simulation blocks. The information related to the parasitic effects also should be provided. In generic tools, the component library is available. The design rule constraints and process are of CMOS micromachining process. The RF MEMS devices are fabricated using custom VLSI processes with Silicon, Aluminum, polysilicon and Silicon nitride. For a given fabrication technology, CAD tools are essential for creating the physical parts. Usually, the final output of CAD system of VLSI CAD tools are mask layouts used in lithographic processes, which is also true for MEMS CAD program. The tool developed here fits into framework illustrated in the Fig.1. The focus of MEMS design is now a days at the device level. The tool developed is aimed at RF shunt switch and RF MEMS inductor only and thus all the individual modules are developed for these devices only.

The tool uses three-dimensional geometry. The three-dimensional meshed models developed by the tool, are shown in Fig. 4 (a) (b) and Fig.6. The solid models can be used for various mechanical and electrical analyses. The tool is also useful for visualization of geometries and has 3-D solid modeling capability. The 3D visualization offers RF MEMS designers a platform for immediately visualizing devices for desired fabrication process without having to wait for the actual fabrication. It enables the designer to see the interaction of different layers of the process being used. It is especially useful in viewing 3-D, out-of-plane, multi-degree-of-freedom RF MEMS structures. With the ability to manipulate the structures in a three-dimensional environment, this package becomes a design checker for undesired hinge binding and travel stops. Thus it becomes an important part of designing movable, out-of plane structures. The important aspect of this type of tool is to construct the model for mechanical and electrical analysis. Besides this visualization is important part of such tool. The micromechanical analysis is performed by creating Finite Element Model of the structure. Numerical analysis includes the meshed device model and solving FEM equations. FEM is a powerful and versatile numerical technique for handling problems involving complex geometries and inhomogeneous media. The FEM is also used here for calculating the electrical parameters such as

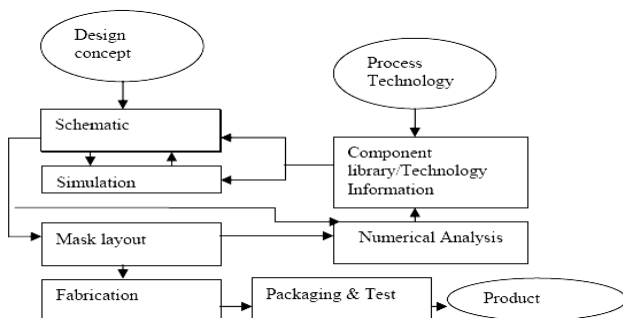


Fig 1 Generic design flow for MEMS

capacitance in this tool. The tool converts the schematic into mask layout in CIF (Caltech Intermediate Form) format. Layout follows design rules of conventional CMOS processes. The CIF net list necessary for planar mask lay out and geometry files are generated by the tool from schematic. The CIF file generated includes information regarding layers and 2D geometrical dimensions. The CMOS fabrication process accepts the CIF file to build masks.

III. RF MEMS shunt switch

MEMS micro switches are receiving increasing attention, particularly in the RF community. Low power consumption, low insertion loss, high isolation, excellent linearity, and the ability to be integrated with other electronics all make micro switches an attractive alternative to other mechanical and solid-state switches. MEMS switches combine the best features of both, having the low control power requirements of FETs, but having “on” resistances and RF insertion losses lower than PIN diodes. Furthermore, MEMS switches have lower off-state capacitance and, as a result, better off-state RF isolation than either FETs or PIN diodes. MEMS switches have inherently high RF linearity. Intended applications include microwave switches that replace PIN diodes and FET switches, while providing lower insertion loss, higher isolation, higher linearity, higher radiation resistance, superior tolerance for high temperature environments, and lower prime power consumption [7]. Example shown here is of MEMS shunt switch. Radio Frequency (RF) MEMS shunt switches offer significant improvements over their macro scale counterparts. These switches exhibit low insertion loss (0.2 dB at 35 GHz) with good isolation (35 dB at 35 GHz). These devices possess on–off capacitance ratios in the range of 75 to 110 with a cutoff frequency in excess of 9000 GHz. The RF MEMS shunt switches are considered here because of their practical utility and extensive use. The Cantilever switch

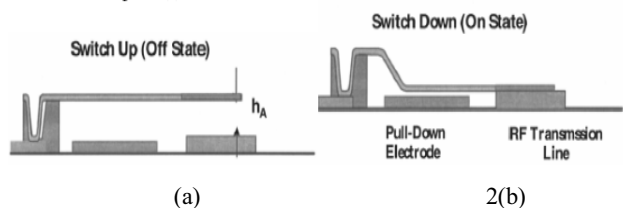


Fig. 2. RF MEMS shunt cantilever switch

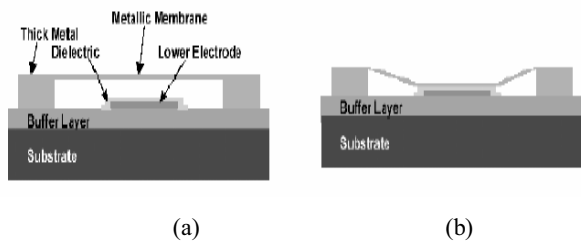
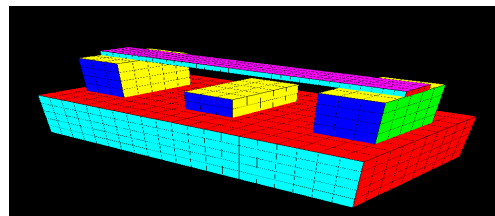
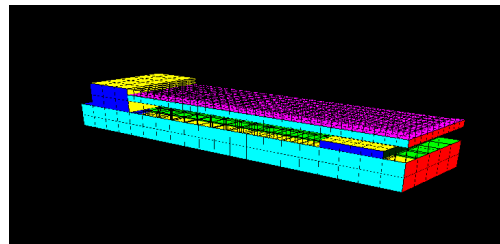


Fig. 3. Multiple supported RF MEMS shunt switch



(a)



(b)

Fig. 4. Meshed models of switch

shown in Fig. 2(a) (b) [8] and multiple supported air bridge shown in Fig. 3(a) (b) [9] are the two common RF MEMS shunt switch structures. The capacitive coupling switches have a thin dielectric film and an air gap between the two metallic contact surfaces. The air gap is electromechanically adjusted to achieve a capacitance change between the ‘up’ (Off) and ‘down’ (On) state. The switches have a movable metal membrane (Aluminum alloy), which pulls down onto a metal/dielectric (Silicon Nitride) sandwich to form a capacitive switch. A typical RF capacitive MEMS switch shown here has 120- $\mu\text{m}$  width, 280- $\mu\text{m}$  length, air gap in the switches 2  $\mu\text{m}$ , the insulator thickness 0.1  $\mu\text{m}$  and its dielectric constant 7 which is developed by Yao [9].

The CAD tool developed here represents these switches as shown Fig. 4 (a) (b). As mentioned earlier the spatiality of this tool is a representation of surfaces. The modeling is done to represent the topology of the surfaces which are formed in the silicon processing. The surface topography is modeled by the scale independent concept of self-similar fractals, which generates the rough surface. The fractal dimension describes the surface roughness and this method is found to be most suitable for surfaces in silicon and other micro-nano technology. The rough surface is modeled using the Mandelbrot-Weierstrass function [10] [11], described by the following equation Eq. (1)

$$f(x) = \sum_{n=-\infty}^{n=\infty} b^{-n(2-D)} [1 - k \cos(b^n x + \phi)] \dots \text{Eq 1}$$

Where fractal dimension,  $D = \log(N)/\log(1/r)$ ,  $r$  is the ratio of  $N$  parts scaled down from the whole,  $b$  is the frequency multiplier value. The parameter  $k$  can be used to alter the profile. By varying  $D$  and  $k$  any profile can be generated. The

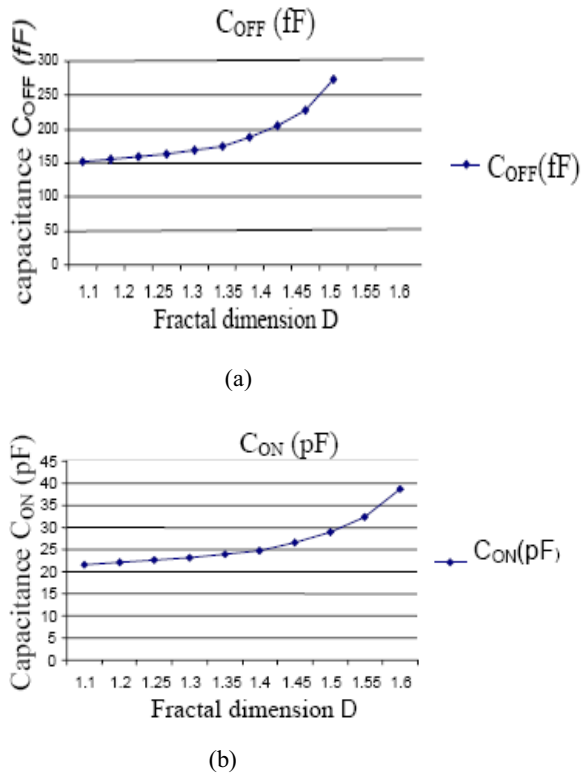


Fig. 5. Variation of capacitance with roughness

electrical properties such as capacitance and electric field for various values of D can be obtained. The capacitance affects insertion loss and isolation. The maximum electric field between two surfaces increases with increase in D, which is a measure of surface roughness. The increase in electric field results into degradation in reliability although it may not suffer breakdown. The capacitance and electric fields are calculated by solving Laplace equation with the finite difference method. The electric field contours and maximum electric field etc obtained from the data. The effect of surface roughness on On, Off capacitance is shown in figure 5(a)(b). A plane strain mechanical model of the RF MEMS switch is adopted to predict the membrane movement. When the voltage is applied between the lower electrode and the metal membrane, the membrane is subjected to the electrostatic force, retaining force of spring and the viscosity force due to the presence of air. The tool generates grid i.e. divides the solution region into finite number of sub regions or elements. After discretization of solution region, the element coefficient matrix and global matrix is calculated. By introducing this variable capacitance in a non-linear circuit solver, the switch performance in terms of distortion can be evaluated. By iteration method the solution is obtained. For mechanical modeling of these devices, the efforts are made to build Finite Element Analysis (FEA) models. The differential equation describing the movement is given by [12]

$$\frac{1}{2} \frac{V^2 \epsilon_0 \epsilon_r S}{[\delta(1/\epsilon_r - 1) + x]^2} - k(x - x_0) - \gamma \dot{x} + \left( e^{-\alpha(x-\delta)} - 1 \right) u(\delta - x) = m \ddot{x} \quad \text{Eq. 2}$$

where  $\epsilon_r$  is relative dielectric constant of Silicon Nitride,  $\delta$  is the thickness of the dielectric,  $V$  is applied switching voltage,  $k$  is spring constant,  $m$  is membrane mass,  $\gamma$  is the air viscosity, parameters  $\alpha$  and  $\beta$  determines the steep of the variation of the repulsive force as function of position,  $x$  is the displacement of membrane. The step function  $u(x)$  ensures that the repulsive force occur only when the plate penetrate the dielectric layer. The solution of Eq. 2 enables to calculate the time varying capacitance of the switch.

#### IV RF MEMS inductor

There are still many functions that cannot be implemented using conventional integrated circuit (IC) technology, in particular, components with high Quality factor Q (exceeding 25), which are required for high-frequency selectivity in communication systems. The advent of VLSI-compatible MEMS fabrication technologies has led to the development of increasingly complex and integrated MEMS based systems. For planar inductors, the parasitic capacitance between the inductor and the ground plane is a problem. To improve the performance, MEMS inductors are proposed to be used high performance systems. The inductor is suspended above the substrate resulting in near to zero parasitic capacitance. A typical MEMS inductor meshed model generated by tool is shown in Fig. 6. A three-dimensional FEM based inductance extractor has been implemented. The nodal voltages are calculated by solving Laplace equation  $\nabla^2 V = 0$  with iteration method using FEM followed by current density computations. The energy of the resulting magnetic field is estimated by integration of Neumann's formula [13]

$$W = \frac{\mu}{8\pi} \int_v \int_v \frac{\vec{J}(\vec{r}) \cdot \vec{J}(\vec{r}')}{|\vec{r} - \vec{r}'|} d^3 r' d^3 r \quad \dots \quad \text{Eq. 3}$$

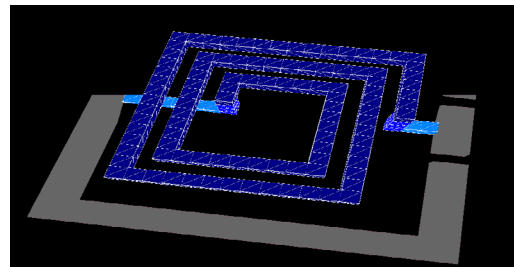


Fig. 6. Meshed model of inductor

where  $v$  denotes the volume of the conductor,  $r$  and  $r'$  denote locations in the volumes. Instead of evaluation of the magnetic vector potential

$$\vec{A}(\vec{r}) = \frac{\mu}{4\pi} \int_v \frac{\vec{J}(\vec{r}')}{|\vec{r} - \vec{r}'|} d^3r' \quad \text{and} \quad \text{calculating}$$

$$W = \frac{1}{2} \int_v \vec{A}(\vec{r}) \cdot \vec{J}(\vec{r}) d^3r$$

with the Gaussian integration scheme, eq (3) is estimated by means of Monte Carlo sampling [14]

$$W \approx \frac{1}{N} \frac{\mu}{8\pi} \sum_i \frac{\vec{J}(\vec{r}) \cdot \vec{J}(\vec{r}_i')}{|\vec{r} - \vec{r}_i'|} \frac{1}{p^2(\vec{r}_i, \vec{r}_i')} = \frac{1}{N} \sum_i W_i \quad \text{Eq 4}$$

During every sample  $i$  two locations  $\vec{r}_i$  and  $\vec{r}_i'$  are chosen

randomly according to the probability density  $p^2(\vec{r}, \vec{r}') > 0$ .

The probability density depends on both locations  $\vec{r}_i$  and

$\vec{r}_i'$  and has to be normalized [15]

$$\int_v \int_v p^2(\vec{r}, \vec{r}') d^3r' d^3r \equiv 1 \quad \dots \text{Eq 5}$$

The inductance  $L$  is computed from  $W$  and the total current through a conductor with [16]  $W = (1/2) L I^2$ . A three turn aluminum inductor with cross section  $85 \mu\text{m} \times 85 \mu\text{m}$  and spacing  $60 \mu\text{m}$  suspended above substrate shown in Fig 6 is analyzed for validation. The inductance offered by the device is  $3.44 \text{ nH}$  which is very close to experimentally observed value [17]. The current density distribution obtained and found is maximum at the inside corners which is expected. The effect of surface roughness is analyzed on scaled inductors with reduced surface to volume ratio of cross sections  $65 \mu\text{m} \times 65 \mu\text{m}$ ,  $50 \mu\text{m} \times 50 \mu\text{m}$ ,  $20 \mu\text{m} \times 20 \mu\text{m}$  and  $3 \mu\text{m} \times 3 \mu\text{m}$ . These values are chosen because most of the inductors are now fabricated in this range now days. The extracted inductances for smooth topology and with surface roughness  $45 \text{ nm rms}$  (fractal dimension  $D=1.51$ ), are shown in Table I. The inductance extracted increases with reducing cross section, with the same length which is also observed experimentally [17].

The effect of micro surface roughness is analyzed. The inductance is extracted for different values of rms roughness. With increase in surface roughness the extracted inductance value increases. The increase in inductance is due to the increased circular current paths inside the volume. The current flowing close to the surface is significantly affected by the rough profile. The crowding of magnetic energy associated

TABLE I

Cross section (micrometer)	Inductance (nH)	
	(smooth topology) L smooth	(45nm rms roughness) L rough
3x3	5.64	6.03
20x20	5.31	5.59
50x50	4.01	4.16
65x65	3.63	3.76
85x85	3.44	3.55

with surface current flow causes the addition in inductance offered.

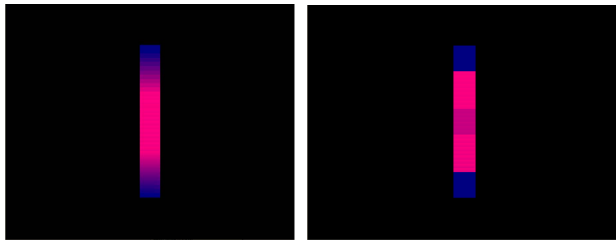
### V. Thermal analysis of RF MEMS shunt switch

For capacitive switches, the primary failure mechanism is stiction between the dielectric layer and the metal since the contact area of the switch is large. The stiction occurs due to dielectric charging within the switch Silicon Nitride layer which is used as dielectric [18]. The electric field can be as high as  $3\text{-}5 \text{ MV/cm}$  in the dielectric layer, which results in a Frankel-Poole charge injection mechanism from the metal to the dielectric resulting charge built-up in dielectric. The trapped charges within the dielectric tend to screen the applied electric fields that are used to control the actuation and release of the switch. This results in the switch being stuck down. It has been observed that the thermal heating due to RF power plays important role in the failure of RF MEMS shunt switches [19]. This paper investigates the effect of the RF power on the steady-state temperature of the switch and its effect on reliability of a capacitive MEMS shunt switch.

A typical RF capacitive MEMS switch discussed in section III and shown in Fig. 3 is considered for analysis. The main mode of heat transfer is due to conduction in the body of switch. The steady state temperature distribution on a MEMS bridge is solved using the generalized heat conduction equation with constant thermal conductivity given by

$$\nabla^2 T + \frac{\dot{g}}{k} = 0$$

where  $T$  is the temperature of the MEMS bridge (degree Celsius),  $\dot{g}$  is the rate of heat generated per unit volume ( $\text{W/m}^3$ ), and  $k$  is the thermal conductivity of the bridge[20]. In the capacitive switch the microwave power induces current in the suspended bridge, which results in Ohmic heating. The power dissipated in the shunt switch is given by  $P = (1/2) I_{\text{rms}}^2 R_s$ , where  $R_s$  is the resistance of the



(a) (b)

Fig. 7 Temperature variation in switch

bridge. The RF power dissipated in the switch in down-state is more than the power dissipated in up-state. It is shown that the temperature of the MEMS bridge does not follow the time-domain RF current. The steady-state analysis is therefore a valid assumption. The computer program developed solves 3-D heat balance equation for steady state conditions with a finite difference numerical solution. The temperature distribution is determined from the solution of the system of governing equations formed by the energy balance equation for conduction thermal mode. The analysis of temperature variation will be useful in the study of reliability and failure mechanism. The Fig. 7(a) shows the temperature variation when the membrane is in up position. (red –hot , blue- cool ). The bridge is cool at supports and hot at centre. In the down position the bridge is cool at centre, Fig. 7(b) because the membrane is in intimate contact with bottom electrode, the heat is transferred to dielectric and finally to lower electrode. The Frankel-Poole mechanism heavily depends on temperature and thus results in leakage current in the dielectric. Since dielectric used is silicon nitride which has high concentration of traps, eventually will result in charging of most of them.

## VI. Summary and Conclusions

As product volume grows and as the time-to-market becomes more crucial, there will be an increasing need for effective design tools that permit experimentation before costly fabrication of MEMS. In this paper tool developed for RF MEMS is described. Performance analysis and failure mechanisms can be addressed by considering effects such as surface roughness, thermal analysis. As the devices are miniaturized the surface micro roughness will play a major role since surface to volume ratio will increase considerably. Development of efficient and accurate CAD will enable design optimization of existing RF MEMS applications. It will also lead to rapid computational prototyping of several innovative applications. The tool will be a valuable tool for the RF MEMS device community.

## References

- [1] Stephen D. Senturia “CAD challenges for Microsensors, Microactuators and Microsystems,” *Proceedings of the IEEE*, Vol. 86, No.8, August 1998, pp 1611-1626.
- [2] T.Ozdemir, K.F.Sabet, J.L.Ebel, G.L.Creech, L.P.B.Katehi, K.Sarabandi, “Numerical modeling of imperfect contacts in capacitively coupled RF MEMS switches.” [www.emagtech.com](http://www.emagtech.com).
- [3] J. R. Reid, “RF MEMS for antenna applications,” Short Course No. 9, *IEEE AP-S Intl. Symp.*, Boston, Massachusetts, June, 2001.
- [4] Gary K. Fedder, “Structured design of Integrated MEMS,” 12<sup>th</sup> IEEE International conference on MEMS, Jan 1999.
- [5] Nicholas R. Swart, “A design flow for micro machined Electro mechanical systems” *IEEE design and test of computers*, Oct-Dec 99.
- [6] John R.Gilbert, “Integrating CAD tools for MEMS design,” *IEEE computer*, April 1998.
- [7] S.Mujamdar, et al., “MEMS Switches,” *IEEE Instrumentation & Measurement Magazine*, March 2003 pp 12-15.
- [8] Elliott R. Brown, “RF-MEMS switches for reconfigurable Integrated circuits,” *IEEE Transactions on microwave theory and techniques*, vol. 46, No. 11, November 1998, pp 1868-1880.
- [9] Jason Yao, “RF MEMS from a device perspective,” *J.Micromech. Microeng.* Vol.10, 2000, pp.R9- R38.
- [10] R.M.Patrikar, Chong Yi Dong, W.Zhuang, “Modeling interconnects with surface roughness,” *Microelectronics Journal* 33(2002)929-934.
- [11] L.Lai, E.A.Irene, J.Vac. “Area evaluation of microscopically rough surface”, *Sci.Technol.* B 17(1999) pp 33-39.
- [12] F. D. Flaviis and R. Coccioli, “Combined mechanical and electrical analysis of microelectromechanical switch for RF applications,” *European Microwave Conference EUMC 1999*, Munich, Germany, 1999, pp 247-250.
- [13] F. Grover, *Inductance Calculations*, Dover Phoenix edition, 1973.
- [14] R.Rubinstein, *Simulation and Monte-Carlo Method*, J.Wiley 1981.
- [15] C.Hoer, C.Love, “Exact inductance equations for Rectangular Conductors with Applications to More Complicated Geometries,” *Journal of research National Bureau of standards* 69C,1965,pp127-37.
- [16] G.Leonhardt, W.Fichtner “acceleration of Inductance Extraction by means of Monte Carlo Method Integrated systems laboratory,” *Swiss Federal Institute of Technology, Gloriastr35*, 8092 Zurich,
- [17] Vijay K. Varadan, K.J.Vinoy and K.A. Jose, *RF MEMS and Their Applications*, John Wiley & Sons, Ltd. 2003.
- [18] C. Goldsmith et al., “Lifetime characterization of capacitive RF MEMS switches,” in *IEEE Int. Microwave Theory and Techniques Symp.*, Phoenix, AZ, May 2001.
- [19] Jonathan Lueke et al. “A Parametric Study of Thermal Effects on the Reliability of RF MEMS Switches,” *International Conference on MEMS, NANO and Smart Systems* July 2005, IEEE Computer Society.
- [20] B. Jensen et al, “Fully integrated electro thermal multiple modeling of RF MEMS switches,” *IEEE microwave & wireless component letters*, vol.13, no. 9, September 2003.